Desalination and Water Treatment
www.deswater.com
doi: 10.1080/19443994.2015.1063463

57 (2016) 7976–7987
April

Taylor & Francis
Taylor & Francis Group

Photocatalytic degradation of cationic dye simulated wastewater using four radiation sources, UVA, UVB, UVC and solar lamp of identical power output

Collin G. Joseph[a,*], Yun Hin Taufiq-Yap[b], Gianluca Li Puma[c], Kogularama Sanmugam[a], Kye Shane Quek[a]

[a]*Sonophotochemistry Research Group, Faculty of Science and Natural Resources, Universiti Malaysia Sabah, 88400 Kota Kinabalu, Sabah, Malaysia, Tel. +6 088 320000, ext. 2117; Fax: +6 088 435324; email: collin@ums.edu.my (C.G. Joseph)*
[b]*Centre of Excellence for Catalysis Science and Technology, Faculty of Science, Universiti Putra Malaysia, 43400 UPM Serdang, Malaysia, Tel. +6 03 89466809; email: taufiq@upm.edu.my*
[c]*Environmental Nanocatalysis & Photoreaction Engineering, Department of Chemical Engineering, Loughborough University, Loughborough LE11 3TU, UK, Tel. +44 0 1509 222510; email: g.Lipuma@lboro.ac.uk*

Received 30 January 2015; Accepted 22 May 2015

ABSTRACT

This study uses photocatalysis, classified under advanced oxidation processes, for the treatment of simulated cationic dye (methylene blue)-contaminated wastewater using TiO_2 as the photocatalyst. Three parameters were manipulated throughout this study including the effects of ultraviolet irradiation wavelength (using UV-A, UV-B, UV-C and solar light), the initial dye concentration (2–10 ppm) and the initial pH (4–10), with a total reaction time of 1 h. The shortest wavelength irradiation (UV-C) proved to be the most effective yielding 100% degradation of MB was achieved within 14 min. Increasing the initial dye concentration reduced the degradation rate due to the inner photon filtering effect by the dye molecules and as a result of the reduced generation rate of hydroxyl radicals. Since MB is a cationic dye, by increasing the pH of the system, the degradation rate was enhanced requiring just 12 min to achieve complete degradation in the experimental photoreactor. This is due to the electrostatic attraction between the dye molecules and the negatively charged TiO_2 particles. Kinetic studies showed that all experiments fulfilled an apparent first-order kinetics at MB concentrations less than 6 pp mmeaning the photocatalytic degradation of MB depended only on its concentration in the solution. Saturation kinetics (zero-order) was observed at MB concentration higher than 6 ppm and a reduction of the initial rate was observed at concentration higher than 10 ppm due the absorption of photon from the dye in solution. From the findings, photocatalysis using TiO_2 is able to fully degrade organic compounds like dyes into degradable substance such as carbon dioxide, water and inorganics.

Keywords: Photocatalysis; TiO_2; Ultraviolet A, B, C irradiation; Solar light irradiation; Methylene blue

---

*Corresponding author.

Presented at the 7th International Conference on Challenges in Environmental Science and Engineering (CESE 2014) 12–16 October 2014, Johor Bahru, Malaysia

1. Introduction

Wastewater from spent dye baths and dye rinsing operations in the textile industry contains many unfixed dyes that may be highly coloured. In terms of wastewater composition and volume discharge, textile wastewater is considered to be the most polluting among all industrial sectors [1]. It was estimated that these industrial dyeing processes lead to an annual discharge of 30,000–150,000 tons of dyes into various receiving water bodies [2].

Kumar et al. [3] reported that most dye-containing effluents from various industrial establishments, mainly dye manufacturing and textile finishing industries are discharged into river waters. In addition, dye wastewaters from the printing industries also sizable sources of environmental contamination, and colour removal is the main problem [4]. The detection of even a miniscule amount of these visible pollutant substances makes it undesirable to the public due to its appearance [5]. Turhan and Ozturkcan [6] have also stated that coloured wastewater damages the aesthetic nature of water and reduces light penetration through its surface, and also the photosynthetic activity of aquatic organisms.

Due to the legislation of new environmental regulations and policies, textile companies are frequently stressed to reduce pollutants and reuse process water and chemicals [1]. This is because textile plants consume large volumes of water and mainstream treatment technologies leave effluents with low biochemical oxygen demand, high chemical oxygen demand and high colour intensities [7]. Since dyes generally have low biodegradability, a conventional biological treatment process is not very satisfactory. Wastewaters containing dyes are usually treated by physical or chemical processes [8]. Such treatments usually include primary treatment such as the removal of suspended solids, followed by a secondary biological treatment process to remove the dissolved or colloidal organic matter [9]. Traditional physicochemical treatment that employs adsorption, coagulation, filtration or ion exchange processes can lead to effective dye decolourization in wastewater. However, such treatment poses further problems such as sludge formation and the processing of the indispensable adsorbent material that needs to be regenerated [10]. In essence, most of these technologies only transfer contaminants from one phase to another without degradation, and the cost for real-scale treatment may needs to be further reduced [11].

Methylene blue (MB) is a cationic dye and it was chosen as the target dye in this study. MB has a wide range of uses, which include dyeing textile materials such as cottons and wools, colouring paper and temporary hair colorant [3]. Although not indicated as a strongly hazardous substance, it may cause various harmful effects. On inhalation, it can give rise to short periods of rapid or breathing difficulties, whereas ingestion through the mouth produces a burning sensation and may cause nausea, gastritis, vomiting and diarrhoea. Accidental large doses induce abdominal and chest pain, profuse sweating, severe headache, mental confusion, painful micturation and methemoglobinemia [12]. Besides that, Anbia and Hariri [8] have also reported that an acute exposure to MB causes increased heart rate, shock, Heinz body formation, cyanosis, jaundice, quadriplegia and tissue necrosis in humans. With regards to these concerns, it is generally thought that cationic dyes are more toxic than anionic dyes [13].

Advanced oxidation processes (AOPs) offer an alternative option for decolorizing and reducing recalcitrant wastewater loadings. AOPs are based on the generation of highly reactive and nonselective hydroxyl radicals in water that can further oxidize organic compounds [14]. AOPs generally show specific advantages over conventional water treatment processes. For instance, the *in situ* generation of strong oxidants may eliminate problems associated with bioresistant organic compounds. Ultimately, the main advantage with AOPs is the ability to mineralize the organic pollutants to CO_2 and H_2O [15]. Among the AOPs, heterogeneous photocatalysis seemed to be an emerging destructive technology that employs semiconductor photocatalysts that are effective in treating refractory organic compounds in water and in particular dyes [16,17].

Photocatalysis [18] is an AOP that uses a photocatalyst (such as anatase-type TiO_2 or ZnO) in the presence of UV radiation (commonly UV-A with a wavelength of 315–400 nm) to degrade pollutants. The main advantage of using semiconductor-based photoactive catalysts materials in the detoxification of pollutants is the complete mineralization of the pollutants into environment-friendly products, without generation of waste, which is not likely to occur in the case of any other treatment method [19]. Photocatalytic reactions show the complete degradation of organic pollutants to very small and not noxious species, without the aid of other chemicals, avoiding sludge production and its disposal [20].

The aim of this project was to study the effects of TiO_2 photocatalysis in the degradation of MB dye in aqueous solution. A parametric study was carried out by manipulating factors such as the irradiation wavelength, the initial dye concentration and the solution pH of the simulated textile wastewater. Reaction kinetics was also investigated with respect to the first-order rate of reaction.

2. Experimental section

2.1. Chemicals and materials

The dye, MB, was purchased from Sigma-Aldrich (≥82%) and used without further purification. HCl and NaOH for pH adjustments, were purchased from Fisher Scientific (37%) and Sigma-Aldrich (≥98%), respectively, and used without further modification.

The photocatalyst used was titanium dioxide (Aeroxide® TiO_2 P25) obtained from Evonik, Germany (formerly known as Degussa). According to the manufacturer's specification, the average primary particle size of the photocatalyst was 21 nm while having a specific surface area (BET) of $50 \pm 15\ m^2/g$. The crystalline components of TiO_2 consist of 80% anatase and 20% rutile. MB is a water-soluble dye which was easily dissolved in distilled water. 1,000 ppm stock solutions were prepared and experimental solutions of desired concentrations were made by successive dilution.

2.2. Photoreactor and light sources

The photoreactor was a batch system (Fig. 1) made by a beaker enclosed in a cabinet to avoid interference from natural light and temperature fluctuations [21]. The radiation sources used for this study were 9W UV-A (365 nm) lamp from Sylvania, 9W UV-B (311 nm) lamp from Philips, 9W (Pro UV, 254 nm) UV-C lamp also from Philips (Model: TUV PL-S 9W/2P 1CT) and 9W Solar (maximum peak at 610 nm) lamp from Coralife. The irradiance from each lamp as supplied by from the manufacturer's specification was $10\ mW/cm^2$. The total radiating surface area was $91.7\ cm^2$ for each individual UV lamp and $86.4\ cm^2$ for the solar lamp. Each lamp was mounted inside a quartz lamp sheath which was immersed in the centre of the beaker reactor [22–26].

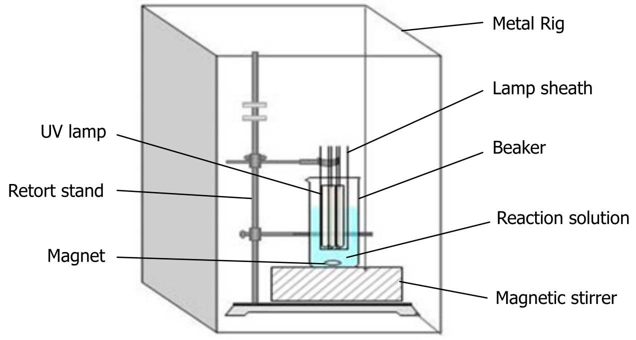

Fig. 1. Schematic diagram of the batch photoreactor.

2.3. Experimental procedure

All control and photodegradation experiments were carried out with 500 mL of solution, at room temperature with continuous magnetic mixing. Control experiments with 4-ppm MB were carried out in the presence of TiO_2 (1 g/L) but in the absence of light, under dark conditions with continuous stirring. Other control experiments carried out in the presence of light irradiation with each lamp source but in the absence of catalyst (photolysis) under similar reacting conditions can be found elsewhere [27]. The experiments in the presence of catalyst were carried out with 1 g/L TiO_2, and with an initial concentration of MB varying between 2 and 10 ppm. The solution pH was adjusted using 0.10 M HCl for acidic pH or 0.10 M NaOH for alkaline pH. All experiments were done in triplicates with their average values being taken and plotted into graphs. Fig. 2 shows the photoreactor set-up using the four different lamp sources.

2.4. Reaction kinetics

The degradation of MB over a time period t was determined from Eq. (1):

$$\%\, D_{\mathrm{deg}} = [(C_0 - C_t)/C_0] \times 100\% \tag{1}$$

where $\%\, D_{\mathrm{deg}}$ is the degradation degree or degradation efficiency; C_0 is the initial concentration of the sample; C_t is the concentration of sample at time, t the time in minutes.

Photocatalytic degradation of dyes generally follows apparent first-order kinetics [19,28,29]. In this study, the first-order rate constant were determined from the linear fitting of a plot of $\ln(C_0/C_t)$ against time (t) according to Eq. (2).

$$\ln\left(C_0/C_t\right) = kt \tag{2}$$

where C_0 is the initial concentration of the sample before illumination; C_t is the concentration of the sample after time t; k is the rate constant; t is the time.

2.5. Analyses

Samples (<3 mL) in each experiment were collected from the reactor every 2 min for the first 20 min and subsequently every 5 min throughout the one hour long experiment. The sample solutions were extracted using a syringe and transferred into vials through a syringe filter (Whatman 0.45 μm membrane filter). The samples were analyzed by UV–vis spectroscopy (Lambda 25 UV–vis Spectrophotometer). The

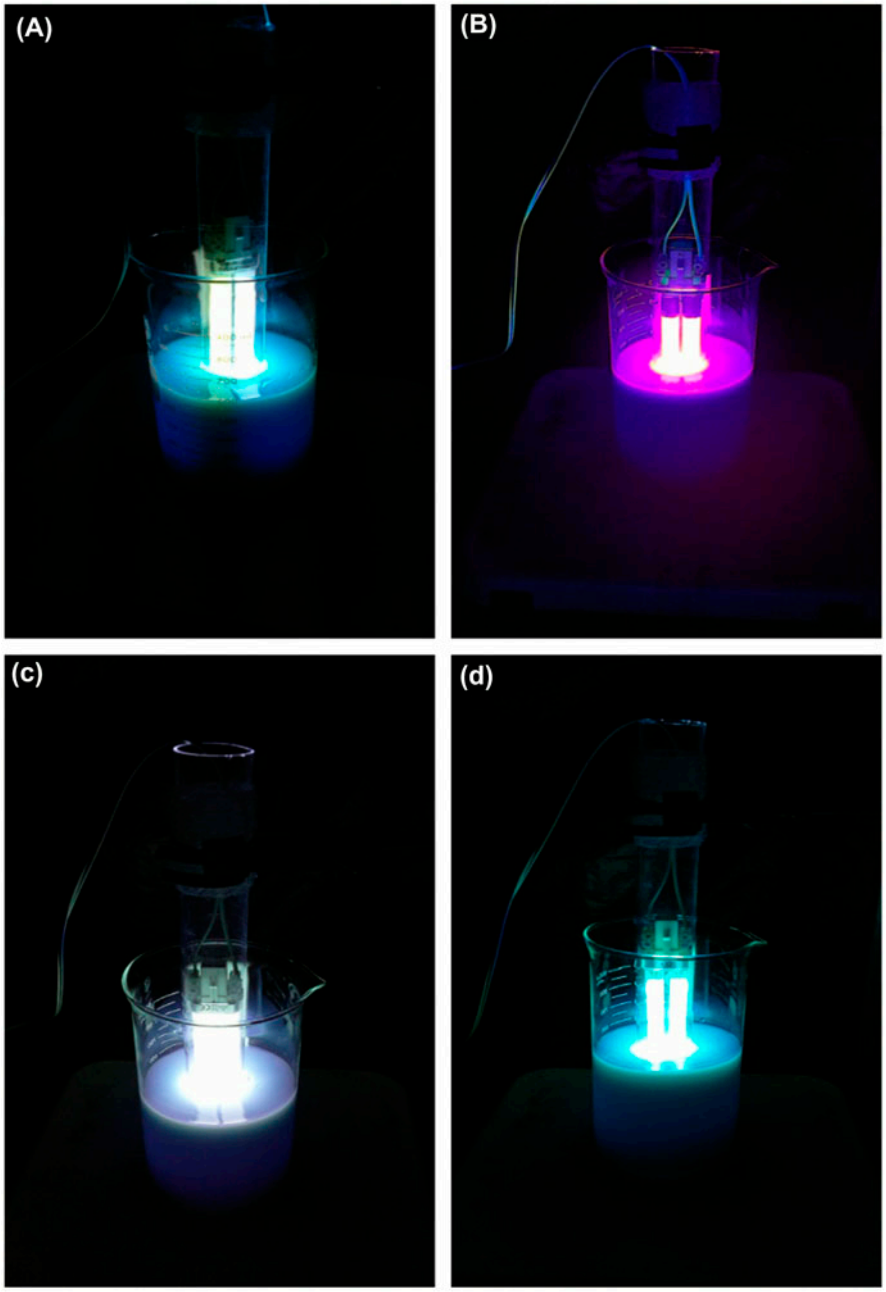

Fig. 2. Batch photoreactor set up for solar (A) UV-A, (B) UV-B, (C) UV-C and (D) lamp.

concentration of MB was determined at the peak absorption at 665 nm from a calibration curve determined using 2, 4, 6, 8 and 10 ppm MB.

3. Results and discussion

3.1. Control experiments

3.1.1. Adsorption on TiO_2

The target pollutant concentration was fixed at 4 ppm. This concentration was chosen because with reference to Beer's Law, the absorbance value for 4 ppm MB is close to 0.435 (the ideal value with least errors) and lies within the range of 0.2–0.7 absorbance units which is within the accepted range that ensures best precision for analytical measurements [30]. The adsorption of MB in the dark onto TiO_2 is shown in Fig. 3.

In the first 25 min, there is a steady yet slight decrease in MB concentration of approximately 5%. After 25 min, the line appears to be fluctuating

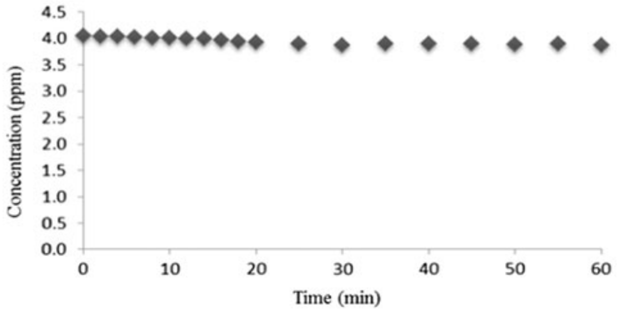

Fig. 3. The adsorption effect of MB on TiO_2 nanoparticles. ([MB] = 4 ppm; TiO_2 (80% anatase, 20% rutile) loading = 1 mg/mL).

signifying that the adsorption–desorption equilibrium was reached. Joshi and Shrivastava [31] reported that 56.4% removal of MB is possible by dark adsorption alone using prepared anatase TiO_2 under MB concentrations within the range of 10–50 ppm at pH 7.0. By comparing with the said findings, it can be concluded that dark adsorption does not play a significant role in this study of photocatalysis using TiO_2.

3.1.2. Photolysis of MB

Fig. 4 shows the photodegradation of MB with different irradiation sources but in the absence of photocatalyst which was published elsewhere [27]. All four types of irradiations showed a decrease in concentration of MB indicating that it undergoes photodegradation.

3.2. Parametric study

3.2.1. Effect of irradiation wavelength

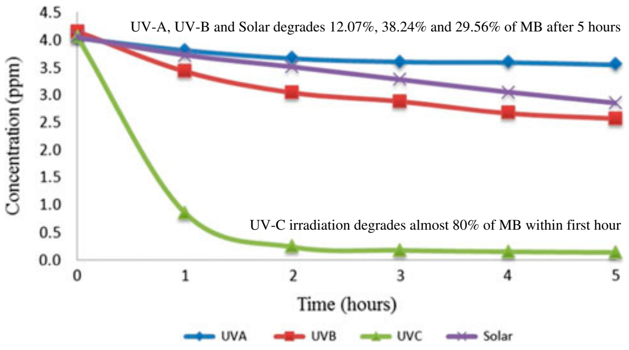

Fig. 4. Photolysis of MB under various light irradiations for 5 h. ([MB] = 4 ppm; TiO_2 loading = none) [27].

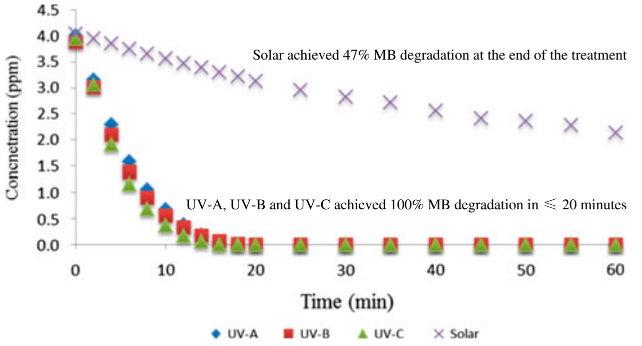

Fig. 5. Photocatalysis of MB using UV-A, UV-B, UV-C and solar lamp. ([MB] = 4 ppm; irradiation time = 1 h; TiO_2 loading = 1 mg/mL).

Fig. 5 shows the results of experiments with different irradiation sources (UV-A, UV-B, UV-C and solar) in the presence of catalyst and at an initial concentration of MB of 4 ppm. UV-C (254 nm) irradiation achieved 100% degradation within the shortest time, which was 14 min. Both UV-B (311 nm) and UV-A (365 nm) irradiation sources were also able to achieve complete degradation but with longer times of 18 min and 20 min, respectively. Solar-assisted photocatalysis proved to be the slowest for MB degradation using TiO_2 photocatalysis.

Solar (610 nm) lamp photocatalysis was unable to achieve 100% degradation within the experimental time limit. The highest degradation efficiency reached with this lamp was 47%. However, since AOPs are a time-dependent treatment and have been reported to achieve complete degradation of pollutant substances, it is expected that solar photocatalysis too may achieve complete photodegradation of MB if the treatment time was increased [32,33].

UV-C irradiation proved to be the most effective, which is most probably due to its capability to induce the direct photolysis action on MB [27,34]. In addition, the shorter penetration capability of UV-C photons into the photocatalyst particle also reduces the probability for electron–hole recombination due to shorter travelling distances leading to greater photocatalytic activity [35]. Fig. 5 shows the UV-vis absorption spectral distortion pattern of MB during the photocatalytic experiments for the four types of light sources used in this study. The maximum absorbance wavelength of each spectral band is marked with a red dot for enhancing the clarity of the observed peak shifts.

From all the absorption spectra (Fig. 6), it is evident that MB under UV and solar irradiation undergoes degradation by photocatalysis. For UV-A, UV-B and UV-C, each subsequent spectral band (from 0 to 60 min) is lower than the other until it completely merges into a vanishing line along the wavelength axis. This demonstrates that photocatalysis using all UV lamps is able to achieve complete degradation. However, such is not the case for solar-induced photocatalysis whereby it is only able to achieve 47% degradation of MB.

From Fig. 6, it is also clearly observable (depicted by red dots) that the $\lambda_{\max}$ for MB is different in each spectra in comparison to the initial value (665 nm). The peaks appeared to be shifted to the left, signifying a hypsochromic (blue) shift. This blue shift is caused by MB undergoing a N-dealkylation process throughout the photocatalytic process [36]. In essence, the auxochromic groups of MB (methyl or methylamine) undergo degradation causing a decrease in the colour intensity [37]. Table 1 suggests the possible intermediates that may be formed during the course of photocatalytic degradation of MB, which explains the blue shift phenomena.

The absorption spectra of MB with photocatalysis using UV-A undergoes a blue shift as much as 39 nm from 665 to 626 nm. For this experiment, the possible demethylated intermediates formed from MB degradation are only AB and then AA. Irradiation of MB under UV-B light also leads to the same intermediates being formed as in UV-A signifying that both these light sources are able to cause partial demethylation of MB. The blue shift was as much as 40 nm with a final $\lambda_{\max}$ to appear at 625 nm. Photocatalysis using UV-C light possibly generated the most number of demethylated intermediates in stages throughout the degradation process that are AB, AA and AC. A blue shift of as much as 57 nm was observed from 665 to 608 nm under UV-C irradiation.

Although UV-C showed the greatest blue shift, it still does not cause MB to undergo complete N-demethylation, which means that thionine may not have been formed. Solar photocatalysis showed the least shift in maximum absorption wavelength with just 7 nm from 665 to 608 nm. The only suggested demethylated intermediate formed for this type of radiation is AB [37].

The bands at 292 and 246 nm for each spectrum can also be seen to decrease significantly with irradiation time without the appearance of new bands. The blue shift was not observed at this wavelength, which suggests that the degradation of MB occurred as a result of the direct breakage of aromatic ring skeletons [36]. It implies that the full oxidative decomposition of the phenothiazine species had occurred and that other intermediates containing the phenothiazine intermediates were no longer formed.

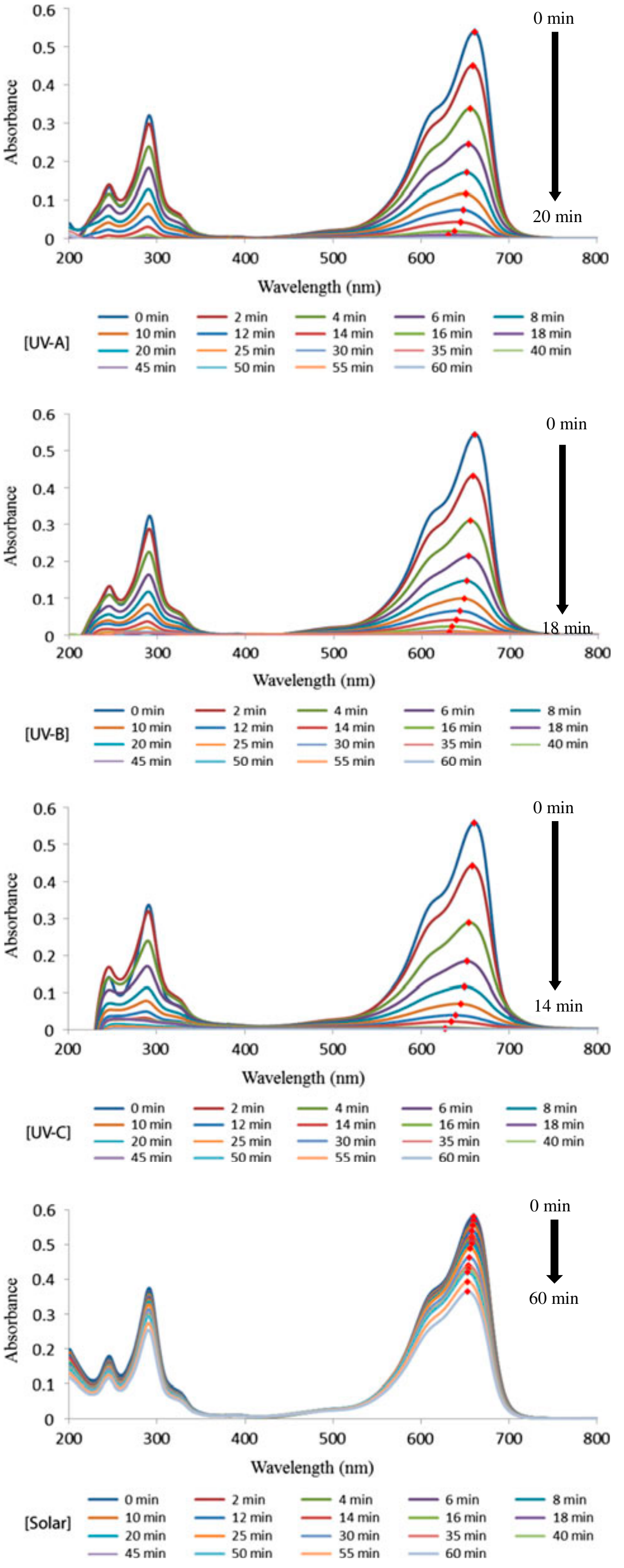

Fig. 6. MB absorption spectral distortion under UV-A, UV-B, UV-C and solar lamp irradiation for 1 h. ([MB] = 4 ppm; TiO_2 loading = 1 mg/mL).

3.2.2. Effect of initial dye concentration

The initial concentration of MB was varied in separate experiments (2, 4, 6, 8 and 10 ppm) with a

Table 1
The structures of possible demethylated intermediates formed which causes the blue shift during MB degradation [37]

Intermediate name and absorption range12	Molecular structure
Azure B (AB) (648–665 nm)	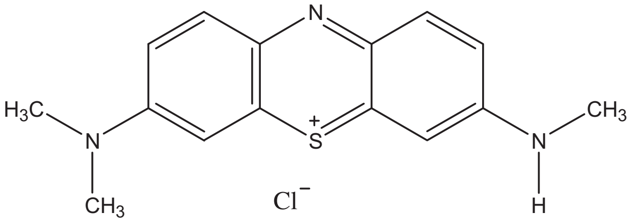
Azure A (AA) (620–634 nm)	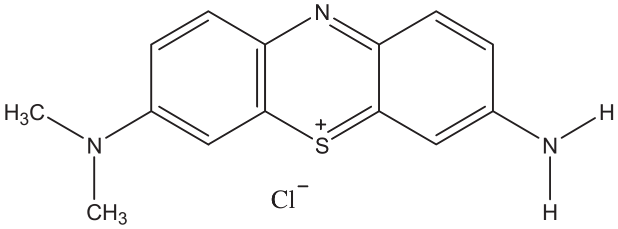
Azure C (AC) (608–612 nm)	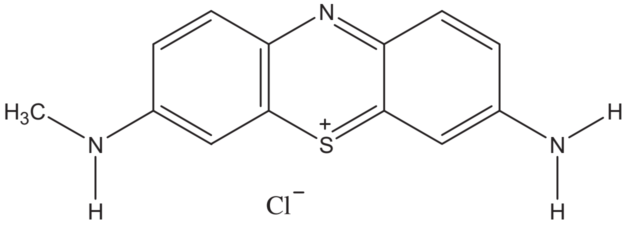
Thionine (Th) (602.5 nm)	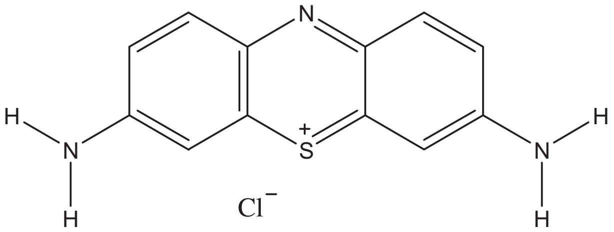

photocatalyst loading was 1 mg/mL. This set of MB concentrations was chosen since it shows good linearity in the UV–Vis absorbance when a calibration curve was plotted ($R^2 = 0.996$). The UV-C light source that gave the fastest removal of MB was selected and the sample was irradiated for 1 h. According to the first-order rate law, increasing the initial pollutant concentration, the degradation rate would increase and the conversion would decrease [38–40]. Fig. 7 shows the effect of initial dye concentration as a function of irradiation time throughout the degradation process.

The degradation rate decreases (gradient becomes less steep) with decreasing initial dye concentration from 10 to 2 ppm.

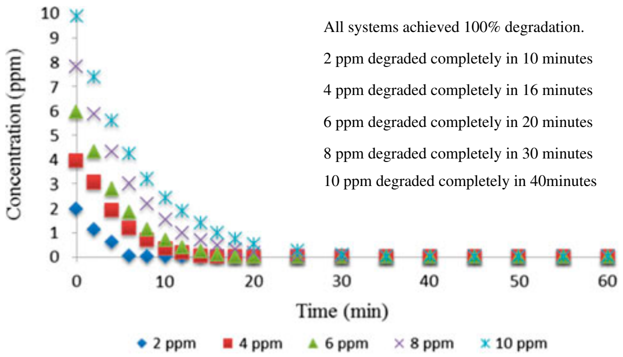

Fig. 7. Photocatalytic degradation of MB under UV-C irradiation for 1 h. ([MB] = 2, 4, 6, 8, 10 ppm; TiO_2 loading = 1 mg/mL).

This observation can be explained in terms of energy wastage. An increase in number of dye molecules per unit volume would lead to an increase in the probability of collision between the dye and hydroxyl radicals. Bearing in mind that the lifetime of a hydroxyl radical is extremely short (few nanoseconds), they can only react as soon as they are formed [41]. Even so, the degradation rate still increases with increasing initial dye concentration until the saturation of the catalyst is reached. The results of the initial rate of reaction shows that the saturation of the catalyst is reached at MB concentration of 6 ppm and higher ions. The results also show that at concentrations of 10 ppm the initial reaction rate decreases as a result of the light-screening effect by the dye itself where light photons are absorbed by the dye molecules and prevented from reaching the photocatalyst surface [39]. The mechanism of dyes absorbing the UV light can be represented by the following reactions (Eqs. (3) and (4)):

$$\mathrm{Dye_{ads}} + h\nu \rightarrow {}^{*}\mathrm{Dye_{ads}} \tag{3}$$

$$ {}^{*}\mathrm{Dye_{ads}} + \mathrm{TiO_2} \rightarrow {}^{\cdot}\mathrm{Dye^{+}_{ads}} + \mathrm{TiO_2}\ (\mathrm{e^-}) \tag{4}$$

The dye (MB) would be capable of charge injection from the excited state of the dye to the conduction band of TiO_2 generating an electron and this may lead to an increase in the generation of superoxide radical anion (${}^{\cdot}O_2^-$) in the presence of adsorbed oxygen on the photocatalyst surface [42]. However, since organic loading is high, it is not likely to have much adsorbed oxygen on the TiO_2 surface and in the absence of suitable scavenger there may be an electron accumulation in the conduction band of TiO_2 leading to an increase in the rate of recombination of e^- and h^+ [19,41,43,44]. As a result, photonic energy would largely be wasted in the form of heat energy according to Eq. (5) which results in a decrease of MB degradation rate.

$$\mathrm{TiO_2}\ (\mathrm{e^-} + \mathrm{h^+}) \rightarrow \mathrm{TiO_2} + \text{ Heat (Dissipated energy)} \tag{5}$$

3.2.3. *Effect of initial solution pH*

In these experiments, the MB initial concentration was kept constant at 4 ppm and the photocatalyst loading was 1 mg/mL. The light source used was UV-C and the irradiation time 1 h. This light source was used for to same reason as explained in Section 3.2.1. The pH range in these experiments was varied in the range 4 to 10 due to practical reasons. To work outside, these values would not be economical if the pH the of wastewater needs to be adjusted to extreme values during industrial applications [45]. The literature suggest that pH is, is a major factor that influences the rate of photocatalytic processes [42,46]. Therefore, it was crucial to determine the optimal pH of reaction for the degradation of MB. Fig. 8 shows the effect of initial solution pH on the TiO_2 photocatalytic degradation of MB.

From Fig. 8, photocatalysis of MB using TiO_2 can be seen to work best under alkaline conditions. Within the fixed time for this study, complete degradation of MB was achieved under all pH conditions but at different rates. In the order of increasing efficiency, pH 4 was the least favourable condition followed by neutral pH (pH 7) and pH 10 was the most favourable condition for MB photocatalytic degradation. This result proved to be in agreement with relevant past studies [16,47].

The pH effect can be explained in terms of electrostatic interaction between the catalyst surface and the target pollutant. The pH influences the surface state of catalyst and the ionization state of ionizable organic compounds thereby affecting the interfacial electron transfer and the photoredox process. The overall photocatalyic degradation can either be enhanced or retarded depending on the dominance of either attractive forces or repulsive forces [42,47,48]. In general, alkaline pH values have been favourable for the photocatalytic degradation of cationic dyes whereas anionic dyes are more readily degraded in acidic conditions [49]. This can be further explained by understanding the zero-point charge concept for semiconductors. The zero-point charge for TiO_2 is known to be at approximately pH 6.8 [40,49,50]. Below or above this value, the surface of TiO_2 can either be positively charged or negatively charged according to Eqs. (6) and (7).

$$\text{When pH} < \mathrm{pH_{zpc}} \quad \mathrm{TiOH} + \mathrm{H^+} \leftrightarrow \mathrm{TiOH_2^+} \tag{6}$$

$$\text{When pH} > \mathrm{pH_{zpc}} \quad \mathrm{TiOH} \leftrightarrow \mathrm{TiO^-} + \mathrm{H^+} \tag{7}$$

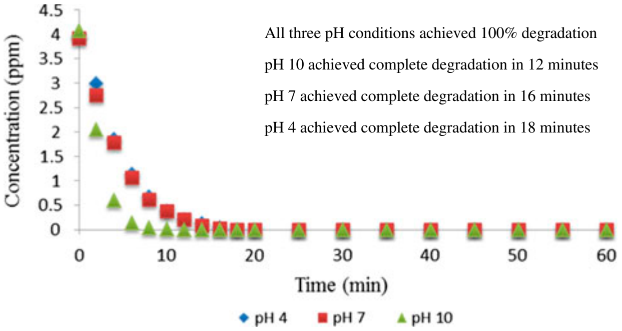

Fig. 8. Photocatalytic degradation of MB using UV-C irradiation under acidic, neutral and alkaline pH. ([MB] = 4 ppm; irradiation time = 1 h; TiO_2 loading = 1 mg/mL).

At alkaline pH (Eq. (7)), more negative charges at the photocatalyst surface cause more MB adsorption or migration of it to be closer to the catalyst surface due to electrostatic interaction since MB is cationic in aqueous solution. Therefore, such conditions would cause the dye to be more susceptible to photodegradation [51]. Not only that, in an alkaline solution, there will be more hydroxide ions available to be oxidized into

·OH on the photocatalyst surface that diffuse to bulk solution leading to an expected enhance in the photocatalytic process [50].

Under neutral conditions, the TiO_2 photocatalyst tends to agglomerate. The zero surface charge yields zero electrostatic surface potential that cannot produce the interactive rejection necessary to separate the particles within the liquid. This induces a phenomenon of aggregation and TiO_2 clusters become larger [45]. Not only that, when TiO_2 agglomerates, surface area available for dye adsorption and photon absorption would be reduced leading to a lower degradation efficiency as compared to alkaline mediums [50].

In an acidic medium, the surface of TiO_2 would be more positively charged (Eq. (6)). Since MB is cationic in nature, the dye would electrostatically repel from being adsorbed on the surface of the photocatalyst leading to the degradation process inhibition [46]. However, degradation does still occur at pH 4, and complete degradation was also achieved although longer irradiation time is needed. It is understood that the positive holes (h^+) are considered as the major oxidation species at low pH and probably a majority of the degradation process underwent based on Eq. (8) [50].

$$h^+ + \text{MB} \rightarrow \text{Degradation compounds} \tag{8}$$

3.3. Kinetic study

Based on literature, the photocatalytic degradation of dyes generally follows apparent apparent the first-order kinetics [19,28,29] until the saturation of the catalyst sutface is reached and the reaction rate become zero order. Furthermore, at very high catalyst concentration the dye molecules reduce the photon flux that reaches the catalyst surface and the reaction rate may even decrease [51]. This behaviour has often been modeled by a rate law resembling the Langmuir-Hinshelwood kinetics [51]. To investigate the reaction kinetics of each parametric study, a graph of $\ln(C_0/C_t)$ against time was plotted. In order to fulfil the requirements for first-order kinetics, the trend line across the plotted points should show a high value of the regression correlation with the gradient returning the rate constant [46]. Based on the results obtained varying each parameter, all the experiments fulfilled first-order kinetics. Table 2 shows the rate constants and the regression correlation for the effect of irradiation wavelength on the photocatalytic degradation of MB.

From the regression correlation values (Table 2), all types of lamps used to study the degradation of MB fit well with the first-order kinetics. UV-C radiation showed the best regression correlation value (0.9901) for this parameter and the highest rate constant ($0.2492\ \text{min}^{-1}$) which proves that UV-C would require the least irradiation time to achieve complete degradation as compared to other types of lamps. A positive relationship between irradiation wavelength and rate constant can be made since the rate constants are in increasing order from solar to UV-C (decreasing wavelength). The shorter the irradiation wavelength, the higher will its rate constant be and hence a higher degradation efficiency. Table 3 exhibits the effect of initial dye concentration on the photocatalysis of MB.

Table 2
The rate constant and regression correlation for the effect of different radiation sources on the degradation of MB in water

Experiment	Rate constant, k (min^{-1})	Regression correlation, R^2
UV-A	0.1984	0.9895
UV-B	0.2483	0.9678
UV-C	0.2492	0.9901
Solar	0.0106	0.9885

The results of the initial rate shows an increase of the rate with MB concentration at low MB concentration, and a saturation kinetics (zero-order in a Langmuir-Hinshelwood rate mechanism) at concentrations of 6 ppm and above. WIth 10 ppm the effect of photon absorption by the dye becomes significant and, as a result, the initial degradation rate appears to decrease. The measurements with the highest precision can be seen that it falls for 4 ppm as it has the highest regression correlation value (0.9736). This supports the theory from Dulski [30] that for best precision in analytical measurements, the absorbance reading should be within the range of 0.2–0.7. A trend can also be seen with the rate constants that by increasing the initial dye concentration, the rate constant decreases. This implies that the degradation rate of MB during

Table 3
The rate constant, the initial rate and regression correlation for the effects of initial dye concentration on the photocatalysis of MB

Experiment (ppm)	Rate constant, k (min^{-1})	Regression correlation, R^2
2	0.5928	0.9351
4	0.2881	0.9736
6	0.2876	0.9544
8	0.2151	0.9665
10	0.1709	0.9682

Table 4
The rate constant and regression correlation for the effects of photocatalysis of MB under different pH conditions

Experiment	Rate constant, k (min^{-1})	Regression correlation, R^2
pH 4	0.2759	0.9490
pH 7	0.3018	0.9638
pH 10	0.6348	0.9891

photocatalysis decreases as the initial dye concentration increases. Similar findings can also be found in literature [38,40,52]. The next table (Table 4) shows the effect of initial solution pH on the degradation of target pollutant via photocatalysis.

From the table above (Table 4), the experiment carried out at pH 10 showed the greatest rate constant (0.6348) and the most reliable regression correlation (0.9891). The lowest rate is under acidic conditions (0.3018) and is followed closely by the rate for reaction under neutral pH (0.3018). From the regression correlation values for all the experiment, it can be concluded that the degradation of MB follows the first-order kinetics regardless of pH conditions within the studied range. From the trend of the increasing rate constants from pH 4 to 10, it can be coined that the photocatalytic degradation of cationic dyes (MB) using TiO_2 increases as the solution pH condition is increased [16].

4. Conclusion

Three parameters were manipulated throughout this study for the photocataly tic degradation of MB. UV-C irradiation proved to be the most effective yielding 100% degradation within 14 min. Blue shifts were also observed in the absorption spectra of the samples during irradiation signifying the formation of reaction intermediates being throughout the photocatalytic process. Increasing the initial dye concentration proved to lower the degradation rate due to inner filter effect by dye molecules and a reduced generation of hydroxyl radicals. Since MB is cationic in solution, increasing the pH of the system led to increased degradation rate (12 min to 100% degradation) given by electrostatic interactions. All photocatalysis reactions fulfilled the first-order kinetics at concentration less than 6 ppm signifying that the rate of MB degradation depends entirely on its concentration in the reacting system. Theoretically, photocatalysis treatment can be used to effectively treat wastewater. However, more intense research needs to be carried out before proposing it for industrial-scale applications.

Acknowledgements

This research was supported by the Centre of Research & Innovation of Universiti Putra Malaysia in collaboration with University Malaysia Sabah (Grant No. RACE0008-ST-2013) and is gratefully acknowledged.

List of symbols

$\% D_{\text{deg}}$	—	degradation degree or degradation efficiency
C_0	—	initial concentration of the sample
C_t	—	concentration of sample at time, t minutes
k	—	rate constant
t	—	time

References

[1] A.R. Tehrani-Bagha, N.M. Mahmoodi, F.M. Menger, Degradation of a persistent organic dye from colored textile wastewater by ozonation, Desalination 260(1–3) (2010) 34–38.

[2] W. Zhao, F. Liu, Y. Yang, M. Tan, D. Zhao, Ozonation of Cationic Red X-GRL in aqueous solution: Kinetics and modeling, J. Hazard. Mater. 187(1–3) (2011) 526–533.

[3] K.V. Kumar, V. Ramamurthi, S. Sivanesan, Modeling the mechanism involved during the sorption of methylene blue onto fly ash, J. Colloid Interface Sci. 284(1) (2005) 14–21.

[4] X. Guo, Y. Yao, G. Yin, Y. Kang, Y. Luo, L. Zhuo, Preparation of decolorizing ceramsites for printing and dyeing wastewater with acid and base treated clay, Appl. Clay Sci. 40(1–4) (2008) 20–26.

[5] V. Vadivelan, K.V. Kumar, Equilibrium, kinetics, mechanism, and process design for the sorption of methylene blue onto rice husk, J. Colloid Interface Sci. 286(1) (2005) 90–100.

[6] K. Turhan, S.A. Ozturkcan, Decolorization and degradation of reactive dye in aqueous solution by ozonation in a semi-batch bubble Column reactor, Water Air Soil Pollut. 224(1) (2013) 1–13.

[7] L.W. Lackey, R.O. Mines Jr., P.T. Mccreanor, Ozonation of acid yellow 17 dye in a semi-batch bubble column, J. Hazard. Mater. 138(2) (2006) 357–362.

[8] M. Anbia, S.A. Hariri, Removal of methylene blue from aqueous solution using nanoporous SBA-3, Desalination 261(1–2) (2010) 61–66.

[9] O.S.G. Soares, J.J. Órfão, D. Portela, A. Vieira, M.F.R. Pereira, Ozonation of textile effluents and dye solutions under continuous operation: Influence of operating parameters, J. Hazard. Mater. 137(3) (2006) 1664–1673.

[10] M. Magureanu, C. Bradu, D. Piroi, N.B. Mandache, V. Parvulescu, Pulsed corona discharge for degradation of methylene blue in water, Plasma Chem. Plasma Process. 33(1) (2013) 51–64.

[11] M.Y. Sun, J. Jin-Oh, L. Heon-Ju, Dielectric barrier discharge plasma-induced photocatalysis and ozonation for the treatment of wastewater, Plasma Sci. Technol. 10(1) (2008) 100.

[12] D. Ghosh, K.G. Bhattacharyya, Adsorption of methylene blue on kaolinite, Appl. Clay Sci. 20(6) (2002) 295–300.

[13] B.K. Nandi, A. Goswami, M.K. Purkait, Removal of cationic dyes from aqueous solutions by kaolin: Kinetic and equilibrium studies, Appl. Clay Sci. 42 (3–4) (2009) 583–590.

[14] S. Sharma, J. Buddhdev, M. Patel, J.P. Ruparelia, Studies on degradation of reactive red 135 dye in wastewater using ozone, Proc. Eng. 51 (2013) 451–455.

[15] P.M.K. Manoj Kumar Reddy, B.R. Rama Raju, J. Karuppiah, E.L. Linga Reddy, C. Subrahmanyam, Degradation and mineralization of methylene blue by dielectric barrier discharge non-thermal plasma reactor, Chem. Eng. J. 217 (2013) 41–47.

[16] A. Houas, H. Lachheb, M. Ksibi, E. Elaloui, C. Guillard, J.M. Herrmann, Photocatalytic degradation pathway of methylene blue in water, Appl. Catal., B: Environ. 31(2) (2001), 145–157.

[17] H. Chun, W. Yizhong, T. Hongxiao, Destruction of phenol aqueous solution by photocatalysis or direct photolysis, Chemosphere 41(8) (2000) 1205–1209.

[18] C.G. Joseph, G. Li Puma, A. Bono, D. Krishnaiah, Sonophotocatalysis in advanced oxidation process: A short review, Ultrason. Sonochem. 16(5) (2009) 583–589.

[19] S.B. Gajbhiye, Photocatalytic degradation study of methylene blue solutions and its application to dye industry effluent, IJMER 2(3) (2012) 1204–1208.

[20] J. Grzechulska-Damszel, M. Tomaszewska, A.W. Morawski, Integration of photocatalysis with membrane processes for purification of water contaminated with organic dyes, Desalination 241(1–3) (2009) 118–126.

[21] C.G. Joseph, G. Li Puma, A. Bono, Y.H. Taufiq-Yap, D. Krishnaiah, Operating parameters and synergistic effects of combining ultrasound and ultraviolet irradiation in the degradation of 2,4,6-trichlorophenol, Desalination 276(1–3) (2011) 303–309.

[22] C.G. Joseph, G. Li Puma, A. Bono, Y.H. Taufiq-Yap, D. Krishnaiah, Sonolysis, photolysis and sequential sonophotolysis for the degradation of 2,4,6-trichlorophenol: The effect of solution concentration, Chem. Eng. Commun. 202(8) (2014) 1061–1068.

[23] PL-S 9W BLB/2P 1CT. Philips Product Catalogue. Available from: <http://www.ecat.lighting.philips.com.my/l/lamps/compact-fluorescent-non-integrated/pl-s/pl-s-blacklight-blue/927901710807_eu/>. Accessed (29 August 2014).

[24] PL-S 9W/01/2P 1CT. Philips Product Catalogue. Available from: <http://www.ecat.lighting.philips.com/l/lamps/special-lamps/medical-lamps/medical-therapy-uvb-narrow-band/uv-b-narrowband-pl-l-pl-s/927901700121_na/>. Accessed (29 August 2014).

[25] TUV PL-S 9W/2P 1CT. Philips Product Catalogue. Available from: <http://www.ecat.lighting.philips.com.my/l/lamps/special-lamps/purificationwater-and-air/residential-water-and-air/tuv-pl-s/927901704007_eu/>. Accessed (29 August 2014).

[26] Replacement Lamp Product Series. Coralife. Available from: <http://www.coralifeproducts.com/product/lamps/>. Accessed (29 August 2014).

[27] C.G. Joseph, Y.H. Taufiq-Yap, L. Elilarasi, K. Vigneswar, Remediation of cationic dye simulated wastewater using photolysis: Parametric and kinetic studies, Malaysian J. Chem. (or MJChem) (2014), (submitted).

[28] L.V. Jian-xiao, C. Ying, X. Guo-hong, Z. Ling-yun, W. Su-fen, Decoloration of methylene blue simulated wastewater using a UV-H_2O_2 combined system, J. Water Reuse Desalin. 1(1) (2011) 45–51.

[29] N. Xu, Z. Shi, Y. Fan, J. Dong, J. Shi, M.Z.C. Hu, Effects of particle size of TiO_2 on photocatalytic degradation of methylene blue in aqueous suspensions, Ind. Eng. Chem. Res. 38(2) (1999) 373–379.

[30] T.R. Dulski, Trace Elemental Analysis of Metals: Methods and Techniques, CRC Press, Basel, 1999.

[31] K.M. Joshi, V.S. Shrivastava, Removal of methylene blue dye aqueous solution using photocatalysis, Int. J. Nano Dimension 2(4) (2012) 241–252.

[32] P.S. Dunlop, T.A. McMurray, J.W. Hamilton, J.A. Byrne, Photocatalytic inactivation of *Clostridium perfringens* spores on TiO_2 electrodes, J. Photochem. Photobiol. A: Chem. 196(1) (2008) 113–119.

[33] J. Zhang, K.H. Lee, L. Cui, T.S. Jeong, Degradation of methylene blue in aqueous solution by ozone-based processes, J. Ind. Eng. Chem. 15(2) (2009) 185–189.

[34] R.W. Matthews, S.R. McEvoy, Photocatalytic degradation of phenol in the presence of near-UV illuminated titanium dioxide, J. Photochem. Photobiol. A: Chem. 64(2) (1992) 231–246.

[35] B. Bayarri, M.N. Abellán, J. Giménez, S. Esplugas, Study of the wavelength effect in the photolysis and heterogeneous photocatalysis, Catal. Today 129(1–2) (2007) 231–239.

[36] J. Ryu, W. Choi, Substrate-specific photocatalytic activities of TiO_2 and multiactivity test for water treatment application, Environ. Sci. Technol. 42(1) (2008) 294–300.

[37] T. Zhang, T. Oyama, A. Aoshima, H. Hidaka, J. Zhao, N. Serpone, Photooxidative N-demethylation of methylene blue in aqueous TiO_2 dispersions under UV irradiation, J. Photochem. Photobiol. A: Chem. 140 (2) (2001) 163–172.

[38] M. Saquib, M. Abu Tariq, M. Faisal, M. Muneer, Photocatalytic degradation of two selected dye derivatives in aqueous suspensions of titanium dioxide, Desalination 219(1–3) (2008) 301–311.

[39] M. Qamar, M. Saquib, M. Muneer, Titanium dioxide mediated photocatalytic degradation of two selected azo dye derivatives, chrysoidine R and acid red 29 (chromotrope 2R), in aqueous suspensions, Desalination 186(1–3) (2005) 255–271.

[40] M. Muruganandham, M. Swaminathan, Photocatalytic decolourisation and degradation of reactive orange 4 by TiO-UV process, Dyes Pigm. 68(2–3) (2006) 133–142.

[41] C. Galindo, P. Jacques, A. Kalt, Photochemical and photocatalytic degradation of an indigoid dye: A case study of acid blue 74 (AB74), J. Photochem. Photobiol. A: Chem. 141(1) (2001) 47–56.

[42] R.J. Wu, C.C. Chen, C.S. Lu, P.Y. Hsu, M.H. Chen, Phorate degradation by TiO_2 photocatalysis: Parameter and reaction pathway investigations, Desalination 250(3) (2010) 869–875.

[43] Z. Jiang, H. Wang, H. Huang, C. Cao, Photocatalysis enhancement by electric field: TiO_2 thin film for degradation of dye X-3B, Chemosphere 56(5) (2004) 503–508.

[44] S. Ahmed, M.G. Rasul, W.N. Martens, R. Brown, M.A. Hashib, Advances in heterogeneous photocatalytic degradation of phenols and dyes in wastewater: A review, Water, Air, Soil Pollut. 215(1–4) (2011) 3–29.

[45] S. Malato, P. Fernández-Ibáñez, M.I. Maldonado, J. Blanco, W. Gernjak, Decontamination and disinfection of water by solar photocatalysis: Recent overview and trends, Catal. Today 147(1) (2009) 1–59.

[46] G.M. Madhu, M.A. Raj, K.V.K. Pai, J. Titamium oxide (TiO_2) assisted photocatalytic degradation of methylene blue, J. Environ. Biol. 30 (2009) 259–264.

[47] A.R. Khataee, M. Zarei, Photocatalysis of a dye solution using immobilized ZnO nanoparticles combined with photoelectrochemical process, Desalination 273 (2–3) (2011) 453–460.

[48] N.P. Mohabansi, V.B. Patil, N. Yenkie, A comparative study on photo degradation of methylene blue dye effluent by advanced oxidation process by using TiO_2/ZnO photo catalyst, Rasāyan J. Chem. 4(4) (2011) 814–819.

[49] I.A. Alaton, I.A. Balcioglu, D.W. Bahnemann, Advanced oxidation of a reactive dyebath effluent: comparison of O_3, H_2O_2/UV-C and TiO_2/UV-A processes, Water Res. 36(5) (2002) 1143–1154.

[50] I.K. Konstantinou, T.A. Albanis, TiO_2-assisted photocatalytic degradation of azo dyes in aqueous solution: kinetic and mechanistic investigations, Appl. Catal. B: Environ. 49 (2004) 1–14.

[51] D. Ollis, C. Gomez Silva, J. Faria, Simultaneous photochemical and photocatalyzed liquid phase reactions: Dye decolorization kinetics, Catal. Today 240 (2015) 80–85.

[52] M. Abu Tariq, M. Faisal, M. Saquib, M. Muneer, Heterogeneous photocatalytic degradation of an anthraquinone and a triphenylmethane dye derivative in aqueous suspensions of semiconductor. Dyes Pigm. 76(2) (2008) 358–365.